Progress In Electromagnetics Research B, Vol. 103, 101–118, 2023

Quantum Illumination Radar Using Polarization States of Photons in Atmosphere: Quantum Information Approach

Sylvain Borderieux*, Arnaud Coatanhay, and Ali Khenchaf

Abstract—The quantum illumination radar uses pairs of entangled photons to enhance the detection sensitivity of a reflecting target. In this paper, we worked on a quantum illumination radar using a pair of entangled photons in polarization in the microwave frequency range in the atmosphere. We studied the quantum information evolution modeling the propagation of a photon in the atmosphere while building two binary decision strategies for the QI radar. We focused on the quantum information evolution showing that the quantum discord representing quantum correlations beyond entanglement could represent an interesting resource to explore for the subject of quantum radar. In addition, we made an approximative estimation of the entanglement survival distance in the atmosphere. Results showed that an optimization should be found to favour the survival of quantum correlations or the signal-to-noise ratios calculated with the binary decision strategy.

1. INTRODUCTION

In a founding article of 2008, Lloyd proposed a new idea of radar system: the quantum illumination (QI) radar [1]. This type of quantum radar can theoretically surpass the sensitivity of a classical radar which uses electromagnetic waves. This QI radar's process is based on the entanglement between two photons of which one is kept inside the radar system while the other propagates toward a reflecting object. The photon is reflected by the object, and it potentially comes back in the radar. QI radar theoretically provides an enhancement in detection sensitivity of a low-reflecting target immerging in a bright thermal noise. Since Lloyd's founding article, more studies have been performed. Theoretical articles provided more information about the potentiality of QI radar (suitable quantum states of photons, QI protocols, theoretical limitations) [2–7]. Experimental articles tried to develop quantum technologies and protocols to build a quantum illumination device [8–14]. Nevertheless, there is currently no QI radar system available. Research around the QI radar is motivated by the quantum advantage in sensitivity. Surprisingly, this quantum advantage seems to be kept despite the entanglement vanishing due to the decoherence during the propagation phase in a perturbative environment. Quantum correlations beyond entanglement could explain this resilience to the propagation [15]. However, in the literature there is a lack of study about the propagation phase and the environment influence in the QI radar. In this paper, we specifically work on this subject using a quantum information theory approach including a propagation model and a decision strategy for the QI radar.

In this work, we study the propagation phase using tools of quantum information theory, and we include a binary decision strategy for the QI radar.

The QI radar uses pairs of entangled photons to work. As we seek for a QI radar in atmosphere, we describe photons as qubits in polarization which is a natural choice in current several quantum information processes [16, 17]. During the propagation phase, the emitted photon interacts with the atmosphere which induces a decoherence of the pair of photons. This decoherence phenomenon destroys

Received 18 May 2023, Accepted 17 August 2023, Scheduled 5 November 2023
* Corresponding author: Sylvain Borderieux (sylvain.borderieux@ensta-bretagne.org).
The authors are with the Lab-STICC CNRS UMR 6285, ENSTA Bretagne, France.

the initial entanglement and quantum correlations. It must be noted that decoherence is less important in microwave range than in optics. Therefore, we focus our work on the microwave frequency range to consider a progressive decoherence. We model the propagation phase using a depolarizing quantum channel acting on the pair of entangled photons. Next, using a simplifying hypothesis between the decoherence of the pair of photons and the attenuation of a classical electromagnetic wave, we give approximate values of entanglement survival distances in atmosphere. To follow the entanglement and quantum correlations during the propagation, we respectively use an entanglement rate and quantum discord [18, 19]. In parallel of the propagation model and quantum information approach, we have built two binary decision strategies in order to study the influence of the entanglement and quantum correlations in the QI radar. The binary decision strategies are designed for the microwave frequency range. The objective is to study the influence of entanglement and discord on the QI radar decision scheme including the propagation phase of the emitted photon in an atmospheric environment.

This paper is organized in four sections. Section 2 gives the description of the QI radar, and it presents the quantum information approach for the quantum radar. Section 3 presents the used propagation model including calculations using tools of quantum information theory. Some of these calculations are given in Appendix A. In Section 4, we present two binary decision strategies in parallel of the propagation model. Both decision strategies take into account the thermal noise and the reflection probability of the object (target). The first strategy is based on Lloyd's decision strategy, and it does not consider the propagation channel influence. The second strategy tries to study the distribution of quantum correlations in the QI radar of three mentioned parameters: thermal noise, reflection probability, and the channel influence. Finally, we conclude in Section 5.

2. DESCRIPTION OF THE QI RADAR ON POLARIZATION STATES

We explain here the principles of a QI radar and introduce the quantum information approach.

2.1. QI Radar on Polarization States

The QI radar protocol is divided is three steps in Figure 1 where we distinguish: emission, propagation and reflection, reception. Step (1) consists in creating a pair of entangled photons inside the radar system. In this paper, we work with polarization states of photons since it is commonly used to create entangled states of photons [20, 21].

Step (2) is divided in two substeps because they occur simultaneously. In step (2.a), photon A is kept inside the radar using a quantum memory while photon S is emitted through the atmosphere in step (2.b). On one hand, the quantum memory protects the quantum state of photon A from any perturbation like a partial measurement. The quantum state of photon A cannot be directly modified. On the other hand, photon S propagates through the atmosphere before being reflected by the object. It potentially comes back to the QI radar to perform the final step. Step (3) is the measurement step. It consists in a joint measurement on the pair of photons AS. Such a measurement supposes to synchronize the storage of photon A with the propagation duration of photon S. Such a synchronization is an experimentally challenging task. Step (3) aims to test the position of the potential target. Thus, we have to build a decision strategy for the QI radar.

In the QI radar, we use a pair of entangled photons AS. We work with two qubits in horizontal and vertical polarization states, respectively, noted as $|H\rangle$ and $|V\rangle$. In the basis of the two qubits $\{|HH\rangle, |HV\rangle, |VH\rangle, |VV\rangle\}$, we consider generalized entangled states $|\Psi^{\pm}\rangle_{\mathrm{AS}} = a|HV\rangle_{\mathrm{AS}} \pm b|VH\rangle_{\mathrm{AS}}$ and $|\Phi^{\pm}\rangle_{\mathrm{AS}} = a|HH\rangle_{\mathrm{AS}} \pm b|VV\rangle_{\mathrm{AS}}$ with the normalization condition $|a|^2 + |b|^2 = 1$ where $a, b \in \mathbb{R}$. We have the quantum states $\{|\Psi^{\pm}\rangle, |\Phi^{\pm}\rangle\} \in \mathcal{H}_{\mathrm{AS}}$, where $\mathcal{H}_{\mathrm{AS}} = \mathcal{H}_{\mathrm{A}} \otimes \mathcal{H}_{\mathrm{S}}$ is the Hilbert space of states for the system AS. To perform the quantum information approach, we use the density matrices

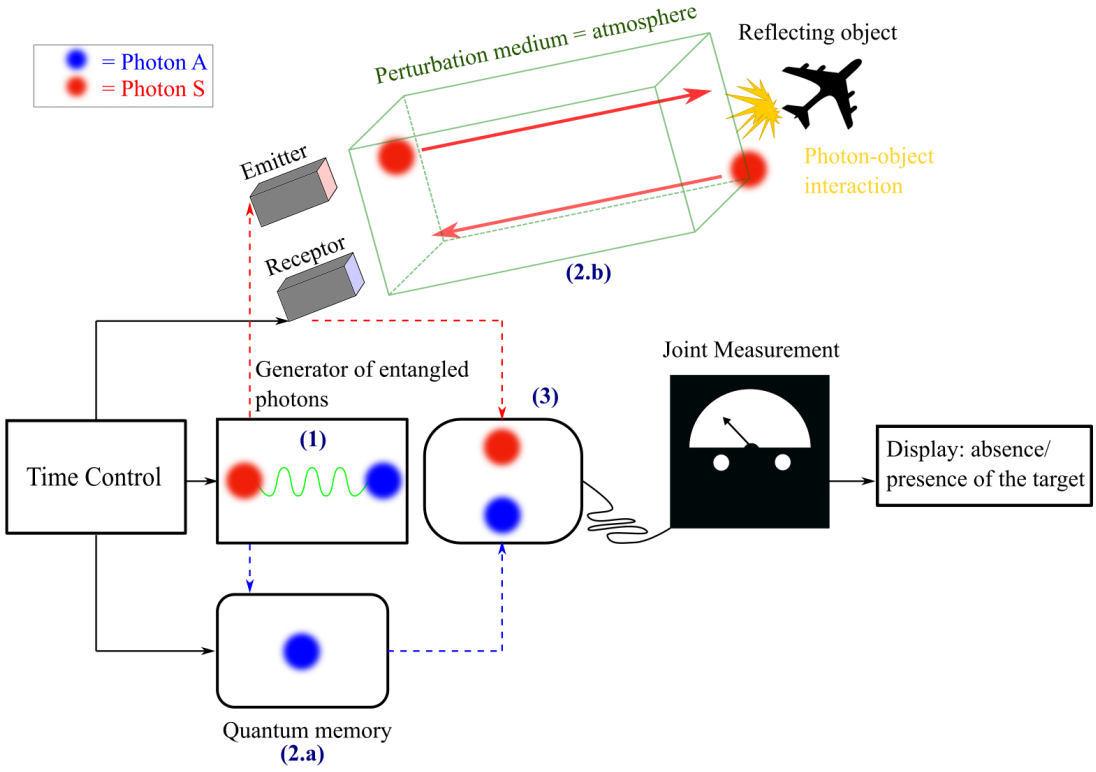

Figure 1. Description of the steps 1–3 of the QI radar protocol which combines a simple illustration of a block diagram with a representation of the QI radar situation in the atmosphere.

$\hat{\rho}_{\mathrm{AS}} \in \mathcal{L}(\mathcal{H}_{\mathrm{AS}})$ in Equation (1) where $\mathcal{L}(\mathcal{H}_{\mathrm{AS}})$ is the space of operators applied to $\mathcal{H}_{\mathrm{AS}}$.

$$\hat{\rho}_{\mathrm{AS}}^{\Psi^{\pm}} = |\Psi^{\pm}\rangle\langle\Psi^{\pm}|_{\mathrm{AS}} = \begin{pmatrix} 0 & 0 & 0 & 0 \\ 0 & a^2 & \pm ab & 0 \\ 0 & \pm ba & b^2 & 0 \\ 0 & 0 & 0 & 0 \end{pmatrix} \tag{1a}$$

$$\hat{\rho}_{\mathrm{AS}}^{\Phi^{\pm}} = |\Phi^{\pm}\rangle\langle\Phi^{\pm}|_{\mathrm{AS}} = \begin{pmatrix} a^2 & 0 & 0 & \pm ab \\ 0 & 0 & 0 & 0 \\ 0 & 0 & 0 & 0 \\ \pm ba & 0 & 0 & b^2 \end{pmatrix} \tag{1b}$$

Note that when $a = b = 1/\sqrt{2}$, we obtain Bell states which are maximally entangled states for the two qubits [17]. The density operators in Equation (1) constitute the starting point of the quantum information approach since they contain all available information about the quantum state of the pair AS. It represents the basic tools to compute the quantum information evolution of our system.

2.2. Quantum Information Approach

For this study, we use tools of quantum information theory to follow the quantum information evolution of the system of photons. For the quantum information approach of the QI radar, we need to make approximations about the target's response and propagation phase.

In this work, the target's response is modeled by a reflection probability $\eta \in [0, 1]$. Note that a theory of Quantum Radar Cross Section (QRCS) currently exists which considers simple geometry shapes (rectangle, disc, triangle) [22]. This model consists in estimating how one incident photon is reflected by a surface in a given direction [23]. The surface is represented by an organized grid of

identical atoms. This QRCS model is built from the sum of interactions of the incident photon with each atom of the grid. Thus, it gives a reflection probability in space depending on the illumination angle. Furthermore, the object QRCS profile would be the same whether we used a pair of entangled photons or single photons to illuminate the target [23]. From the point of view of quantum information theory, the QRCS does not add information about the entanglement evolution or the quantum correlation evolution. Consequently, we do not explicitly refer to the object's shape. If we seek a phenomenological approach of the photon-object interaction, we must use the Quantum Electrodynamics Theory (QED). This is a very complex task. Such a study is not in the scope of this paper, so we have chosen to only describe the photon-object interaction using a reflection probability.

In step (2.b) in Figure 1, we only send one photon to probe a region of atmosphere where there is potentially a object. During its propagation, the emitted photon can be absorbed or scattered by an atmospheric molecule. If photon S is absorbed, the entanglement of the pair AS is destroyed. In the same way, if photon S is scattered by a molecule, it will propagate to infinity and could be absorbed by another molecule later. In both cases, photon S cannot return to the QI radar. As a result, photon S is lost from the QI radar point of view. The total loss of information exactly corresponds to what exists in electromagnetic physics. In this article, we focus more specifically on the progressive loss of information of the pair of entangled photons AS during the propagation phase of photon S. To follow this evolution, we must suppose that photon S is not absorbed or scattered by atmospheric molecules during the propagation. This is an important simplifying hypothesis. Nevertheless, photon S interacts in the atmosphere which modifies the quantum state of the system AS. This decoherence phenomenon destroys the initial entanglement and quantum correlations. We follow the entanglement rate with a measure of entanglement and the rate of quantum correlations thanks to the quantum discord (see Section 3). Note that they are two different quantities. A quantum system can have a non-zero discord while the entanglement measure is zero.

In his article, Lloyd assumed that the initial entanglement is instantly lost in the environment [1]. In optics, this is a suitable approximation. However, decoherence is less important in the microwave frequency range. Therefore, we can make the hypothesis that decoherence is low enough to follow the quantum information evolution. To model the propagation in the atmosphere, we use a depolarizing quantum channel on the pair of photons AS.

In the next section, we explain the propagation model in the atmosphere and the calculations using quantum information theory.

3. PROPAGATION MODEL

In this section, we present the propagation model of photon S in the atmosphere using a parametric quantum channel. We present calculations of the entanglement rate and the quantum discord using the channel parameter. Using this propagation channel, we show how to link it to a classical attenuation in order to give approximative survival distances of entanglement in the atmosphere.

In the QI radar protocol, only one photon is emitted, namely photon S. During its propagation, photon S interacts with the atmosphere. It produces a decoherence phenomenon destroying the initial entanglement of the pair of photons AS. To model the atmosphere action, we use a generalized depolarizing quantum channel $\mathcal{N}$ defined by [24–27]:

$$\mathcal{N}(\hat{\rho}_{\mathrm{AS}}) = \sum_{i=1}^{4} \hat{K}_i \hat{\rho}_{\mathrm{AS}} \hat{K}_i^{\dagger} \tag{2}$$

The Kraus operators $\{\hat{K}_i\}_{i=1\ldots4}$ define the action of the propagation environment on the quantum state $\hat{\rho}_{\mathrm{S}}$ verifying the completeness condition $\sum_{i=1}^{4} \hat{K}_i^{\dagger}\hat{K}_i = \hat{I}$. Note that these operators only act on photon S, not on photon A:

$$\hat{K}_1 = \sqrt{1-\gamma}\left(\hat{I}_{\mathrm{A}} \otimes \hat{I}_{\mathrm{S}}\right) \qquad \hat{K}_2 = \sqrt{\frac{\gamma}{3}}\left(\hat{I}_{\mathrm{A}} \otimes \hat{\sigma}_{x,\mathrm{S}}\right) \tag{3a}$$

$$\hat{K}_3 = \sqrt{\frac{\gamma}{3}}\left(\hat{I}_{\mathrm{A}} \otimes \hat{\sigma}_{y,\mathrm{S}}\right) \qquad \hat{K}_4 = \sqrt{\frac{\gamma}{3}}\left(\hat{I}_{\mathrm{A}} \otimes \hat{\sigma}_{z,\mathrm{S}}\right) \tag{3b}$$

In Equation (3), the parameter $\gamma \in [0,1]$ is the strength of atmospheric influence on the system AS. The matrices $\hat{\sigma}_x, \hat{\sigma}_y, \hat{\sigma}_z$ are Pauli matrices acting on $\hat{\rho}_{\mathrm{S}}$. Applying the depolarizing quantum channel on the quantum states (1a) and (1b), we obtain:

$$\hat{\rho}^{\Psi^{\pm}}_{\mathrm{AS,out}} = \begin{pmatrix} \frac{2}{3}\gamma a^2 & 0 & 0 & 0 \\ 0 & (3-2\gamma)\frac{a^2}{3} & \pm(3-4\gamma)\frac{ab}{3} & 0 \\ 0 & \pm(3-4\gamma)\frac{ab}{3} & (3-2\gamma)\frac{b^2}{3} & \\ 0 & 0 & 0 & \frac{2}{3}\gamma b^2 \end{pmatrix} \tag{4a}$$

$$\hat{\rho}^{\Phi^{\pm}}_{\mathrm{AS,out}} = \begin{pmatrix} (3-2\gamma)\frac{a^2}{3} & 0 & 0 & \pm(3-4\gamma)\frac{ab}{3} \\ 0 & \frac{2}{3}\gamma a^2 & 0 & 0 \\ 0 & 0 & \frac{2}{3}\gamma b^2 & 0 \\ \pm(3-4\gamma)\frac{ab}{3} & 0 & 0 & (3-2\gamma)\frac{b^2}{3} \end{pmatrix} \tag{4b}$$

where Equations (4a) and (4b) are defined as functions of γ. The density matrices $\hat{\rho}^{\Psi^{\pm}}_{\mathrm{AS,out}}$ and $\hat{\rho}^{\Phi^{\pm}}_{\mathrm{AS,out}}$ contain all information about the quantum state of the pair AS. Using the parametric quantum channel, we calculate the entanglement rate and the quantum correlation rate.

The entanglement rate $\mathcal{E}(\hat{\rho}_{\mathrm{AS,out}})$ is calculated with the entanglement of formation using the concurrence of Wootters $\mathcal{C}(\hat{\rho}_{\mathrm{AS,out}})$ [28]. We have calculated the square-roots of eigenvalues $\{\lambda_R^{(i)}\}_{i=0\ldots3}$ of the spin-flip matrix $R = \hat{\rho}_{\mathrm{AS,out}}(\hat{\sigma}_y \otimes \hat{\sigma}_y)\hat{\rho}^{*}_{\mathrm{AS,out}}(\hat{\sigma}_y \otimes \hat{\sigma}_y)$ where $*$ is the complex conjugate, to obtain the concurrence of Wootters:

$$\mathcal{C}(\hat{\rho}_{\mathrm{AS,out}}) = \max\left(0, \sqrt{\lambda_R^{(2)}} - \sqrt{\lambda_R^{(1)}} - \sqrt{\lambda_R^{(1)}} - \sqrt{\lambda_R^{(3)}}\right) = \max\left(0, 2ab(1-2\gamma)\right) \tag{5}$$

where $\lambda_R^{(1)}$ has a multiplicity 2, and $\lambda_R^{(2)}$ and $\lambda_R^{(3)}$ have a multiplicity 1. The concurrence $\mathcal{C}(\hat{\rho}_{\mathrm{AS,out}}) \in [0,1]$ is used in the binary entropy $h(x) = -x\log(x) - (1-x)\log(1-x)$ with $x = (1+\sqrt{1-\mathcal{C}^2(\hat{\rho}_{\mathrm{AS,out}})})/2$ to express the entanglement rate $\mathcal{E}(\hat{\rho}_{\mathrm{AS,out}}) \equiv h(x)$ as function of γ in Figure 2.

Next, we compute the quantum correlation rate using the quantum discord $\delta(\hat{\rho}_{\mathrm{AS,out}})$ defined by [18, 29]:

$$\delta(\hat{\rho}_{\mathrm{AS,out}}) = \min_{\{\hat{M}_{\mathrm{S}}^{(i)}\}} \left[\mathcal{I}(\hat{\rho}_{\mathrm{AS,out}}) - \mathcal{J}(\hat{\rho}_{\mathrm{AS,out}})\right] \tag{6a}$$

$$= \min_{\{\hat{M}_{\mathrm{S}}^{(i)}\}} \left[\overbrace{\mathcal{S}(\hat{\rho}_{\mathrm{A,out}}) + \mathcal{S}(\hat{\rho}_{\mathrm{S,out}}) - \mathcal{S}(\hat{\rho}_{\mathrm{AS,out}})}^{\mathcal{I}(\hat{\rho}_{\mathrm{AS,out}})} - \underbrace{\left(\mathcal{S}(\hat{\rho}_{\mathrm{A,\,out}}) - \mathcal{S}(\hat{\rho}_{\mathrm{A,\,out}}|\hat{\rho}_{\mathrm{S,\,out}})_{\{\hat{M}_{\mathrm{S}}^{(i)}\}}\right)}_{\mathcal{J}(\hat{\rho}_{\mathrm{AS,out}})}\right] \tag{6b}$$

where $\mathcal{I}(\hat{\rho}_{\mathrm{AS,out}})$ is the quantum mutual information, and $\mathcal{J}(\hat{\rho}_{\mathrm{AS,out}})$ is the classical information obtained by projection measurements $\{\hat{M}_{\mathrm{S}}^{(i)}\}_{i=H,V}$ on the subsystem S [19]. Quantum discord represents quantum correlations inside a system. It comes from the difference of the two definitions of mutual information. In classical information theory, mutual information is written $I(X;Y) = I(Y|X)$ for two random variables X and Y. In quantum information theory, these two definitions are no longer equal because we introduce a quantum measurement on the system. Hence, quantum discord depends on the choice of measurements on one of the subsystems A or S. Equation (6b) is the quantum discord $\delta(\hat{\rho}_{\mathrm{AS,out}})$ when measurements are done on the subsystem S. It is represented in Figure 2. The calculations of Von Neumann entropies of Equation (6b) are detailed in Appendix A.

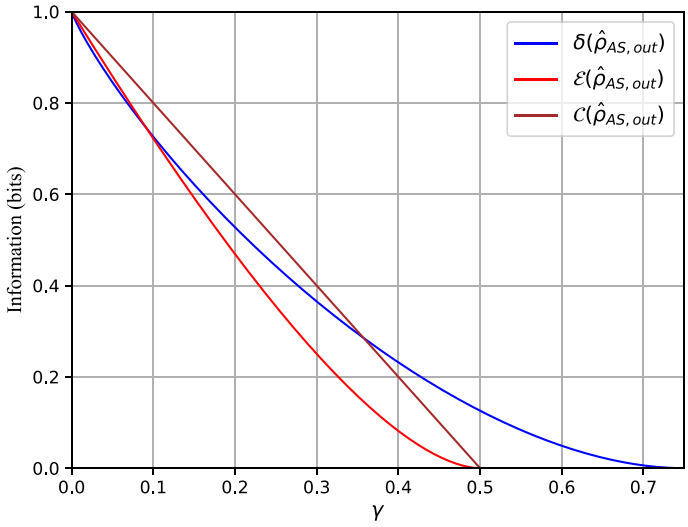

Figure 2. Concurrence of Wootters $\mathcal{C}(\hat{\rho}_{\mathrm{AS,\,out}})$, entanglement of formation $\mathcal{E}(\hat{\rho}_{\mathrm{AS,\,out}})$ and quantum discord $\delta(\hat{\rho}_{\mathrm{AS,out}})$ as function of the damping parameter $\gamma \in [0, 3/4]$.

In Figure 2, we observe the entanglement rate decay and quantum discord decay as function of γ. The quantum correlation rate vanishes when $\gamma = 3/4$ while the entanglement rate already equals zero for $\gamma = 1/2$. Hence, some quantum correlations survive longer than the entanglement to the depolarizing channel action on the system AS. The range validity of the propagation model ends at $\gamma = 3/4$ because from there the behavior of quantum correlations does not represent a consistent physical situation.

Now, using the quantum channel and a simplifying hypothesis of the photon-atmosphere interaction we can estimate the survival distance for the entanglement and for the quantum discord in atmosphere.

The decoherence phenomenon comes from a progressive coupling between photon S and the different molecules in the atmosphere (N_2, O_2, H_2O, etc.) The channel parameter γ in Equation (3) is linked to this coupling. We assume that the damping parameter γ depends on time, so we write it as $\gamma = 1 - e^{-\kappa t}$ [24]. The parameter κ represents the photon-atmosphere coupling, and it depends on the atmosphere nature and the emission frequency of the QI radar. To estimate the coupling, we suppose that κ traduces the density of interactions on the subsystem S with the ensemble of molecules in the atmosphere. These molecules represent an ensemble of scatterers for the incident photon. We can describe interactions between photon S and the molecules by the coupling between photon S and an ensemble of harmonic oscillators in Figure 3. After a given propagation time, the initial entanglement of the pair of photons AS disappears. Here, we consider a mean of all interactions with the different molecules in the atmosphere to avoid a phenomenological study of the decoherence phenomenon. Please note that setting a value to κ is theoretically and experimentally challenging. However, it is possible to give an estimation in order to give a trend for the survival distance of entanglement in the atmosphere.

We make a simplifying hypothesis that the density of interactions is roughly proportional to the classical attenuation of an electromagnetic wave in the microwave range. The parameter κ now depends on atmospheric characteristics (temperature and absorption spectrum) as function of time t. Assuming this proportionality link, we can write $\kappa = L_C \mathcal{A} c$ where $\mathcal{A}$ is the attenuation in $\mathrm{dB.km^{-1}}$, and c is the speed of light. The factor L_C is a proportionality coefficient. We arbitrarily set $L_C = 1$. Then, we obtain the parameter γ as function of the propagation distance x: $\gamma \approx 1 - e^{-\mathcal{A}ct} = 1 - e^{-\mathcal{A}x}$. The classical attenuation in the atmosphere is estimated thanks to the MPM model[†]. As an example, we plot an attenuation spectrum in Figure 4 using the MPM model.

From the parametric quantum channel, we can estimate the survival distance of the entanglement and of the quantum correlations in the atmosphere. In our current model, the entanglement rate and quantum discord respectively vanish for $\gamma_{\mathrm{lim}} = \{1/2, 3/4\}$. To make an estimation of the survival

[†] This model is called MPM for "Millimeter-Wave Propagation Model" from the article [30].

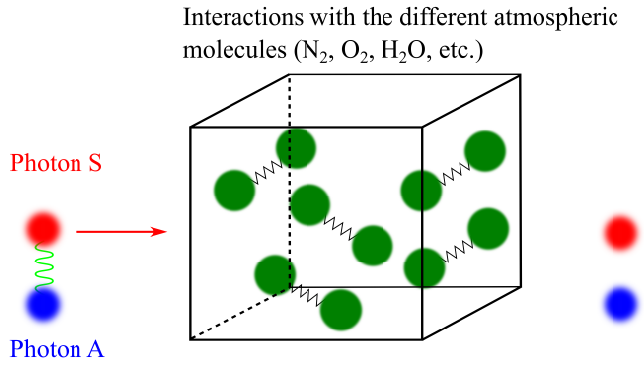

Figure 3. Density of interactions on photon S during the propagation phase inducing the initial entanglement loss. The pair of photons AS is initially entangled on the left. During the propagation, photon S interacts with the atmospheric molecules (N_2, O_2, H_2O, etc.) that destroys entanglement. At the end of the propagation phase, we get a not-entangled pair of photons on the right.

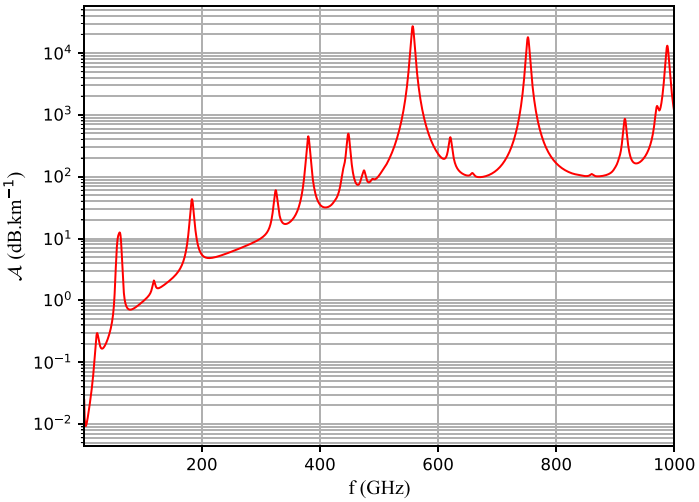

Figure 4. Attenuation $\mathcal{A}$ as function of frequency $f \in [1, 1000]$ GHz, calculated from the MPM model with $T = 300$ K, a humidity rate of 50% and a pressure of 101.3 kPa.

distance, we write:

$$x_{\max} = -\frac{\ln|\gamma_{\lim} - 1|}{\mathcal{A}} \tag{7}$$

Using the MPM model to calculate the attenuation $\mathcal{A}$ (Figure 4), we have plotted the maximal survival distance $\mathcal{E}(\hat{\rho}_{\mathrm{AS,out}}) = 0$ and $\delta(\hat{\rho}_{\mathrm{AS,out}}) = 0$ as function of the emission frequency $f \in [1, 1000]$ GHz in Figure 5. We present the direct calculus (solid lines) and an evolution trend (dashed lines). These curves show a trend for the survival distance since we must not consider the absorption peaks of the MPM model built with the absorption spectra of O_2 and H_2O. As we said before, we consider a mean of photon-atmosphere interactions during the propagation phase. We observe that the survival distance $x_{\max}$ of the entanglement rate and discord quickly drop when the emission frequency increases. Considering Figure 5, we should choose an emission frequency range approximately below 100 GHz to maximize the survival distance of the entanglement and quantum discord.

As an example, for an emission frequency of $f = 5$ GHz, the entanglement vanishes for $x \approx 70$ km whereas the quantum discord vanishes for $x \approx 140$ km. For $f = 10$ GHz, we have a vanishing entanglement at $x \approx 35$ km and a vanishing discord at $x \approx 70$ km. To compare with the current

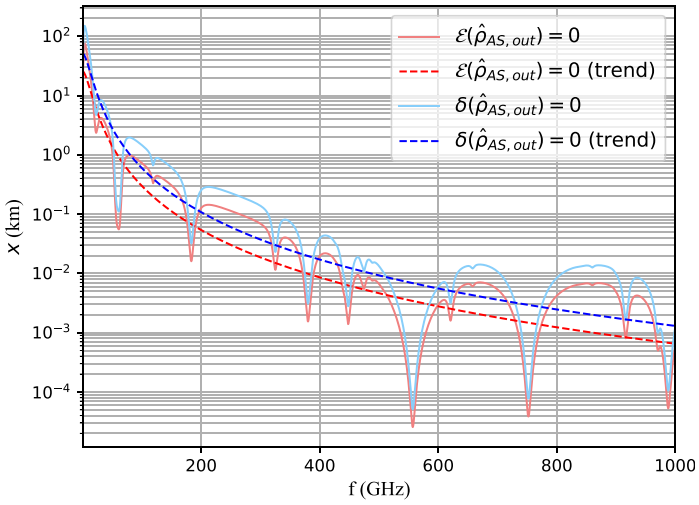

Figure 5. Survival distances $x_{\max}$ for the entanglement rate $\mathcal{E}(\hat{\rho}_{\text{AS,out}})$ and the quantum discord $\delta(\hat{\rho}_{\text{AS,out}})$ using the attenuation model MPM with the same parameters as Figure 4. Solid lines represent calculations using raw datas from the MPM model. Dashed lines represent the evolution trend of entanglement rate and discord obtained with the continuum of the spectrum calculated in Figure 4. This continuum has been obtained excluding the attenuation range above 1 dB.km^{-1} including most of absorption peaks to consider a mean of interactions between the incident photon and the atmosphere. Numerical calculations have been made using Astropy and Specutils packages of the programming language Python.

literature, another article performed a similar study using a phenomenological approach with a master equation [31]. They found a vanishing entanglement around 85 km for an emission frequency of $f = 5$ GHz [31]. Compared to our results, we are in the same order of magnitude keeping in mind that our model is quite simple because this is not a strict phenomenological approach. Indeed, we did not model all interaction phenomena between the emitted photon and atmospheric molecules since we consider a mean of all interactions represented by the parameter γ. The common thread with [31] is the coupling coefficient with the propagation environment which depends on the classical atmospheric attenuation $\mathcal{A}$. However, note that they used an approach based on the continuous variable formalism which consists in describing photons as states of the quantum electromagnetic field [32]. In this paper, we work with the standard formalism of quantum information theory with discrete states [16, 17]. Despite these differences, we obtain the same order of magnitude for the survival distance of entanglement in the atmosphere. Although our propagation model is relatively simple, our results are consistent with the scientific literature.

The propagation model only shows the entanglement loss in the atmosphere. However, in a QI radar we need a decision strategy to detect a target. We present the decision strategies in the next section.

4. DECISION STRATEGIES FOR THE QI RADAR

Here, we focus on the binary decision strategy. Currently, we only use a binary decision strategy which consists in choosing if there is an object or not in the environment. In this paper, we use two binary decision strategies based on Lloyd's binary decision strategy [1, 33].

The first binary decision strategy in Section 4.1 considers the reflection probability of the object and thermal noise. However, it does not take into account the propagation channel influence. The second binary decision strategy in Section 4.2 tries to consider at once three parameters: the reflection probability of the object, the thermal noise, and the channel influence. The objective is to find links between the decision strategy and the survival of quantum correlations during the propagation phase.

4.1. Standard Binary Strategy

This first binary decision strategy has been built in parallel of the propagation model. It does not take into consideration the progressive disentanglement induced by the propagation environment.

The binary decision strategy relies on two hypotheses H_0 and H_1 which respectively correspond to the absence and presence of a reflecting target in the atmospheric environment. We include two parameters in this decision scheme. The first is the reflection probability of the object $\eta \in [0, 1]$ because we assume to not use the QRCS theory. The second is the thermal noise which represents all thermal photons in a given emission frequency of the QI radar. As we use qubits in polarization states to describe the quantum state of photons $\hat{\rho}_{\mathrm{AS}}$ in Equation (1), we model the thermal noise as an ensemble of qubits $\hat{\rho}_B$ in polarization states following a Bose-Einstein law $n(\omega_i, T) = (e^{\beta\hbar\omega_i} - 1)^{-1}$. In this expression, ω_i is the frequency, and the factor $\beta = (k_B T)^{-1}$ depends on temperature T and Boltzmann constant k_B. We write the hypotheses H_0 and H_1 below.

In hypothesis H_0, there is no object. The emitted photon S indefinitely propagates without being reflected by the object. In practice, it can be either absorbed or scattered by atmospheric molecules which means that the initial quantum correlations are lost. From the QI radar point of view, we have lost this photon since it cannot come back in the receiver. In the case where the radar detects something, we assume that the radar detects one photon per detection event, and it only sees one photon from the thermal noise. We make the assumption that this photon has the same quantum state $\hat{\rho}_B = \hat{\rho}'_{\mathrm{S}}$ of the emitted photon. As the thermal noise follows a Bose-Einstein law, the QI radar can detect one thermal photon with a probability $p = 1/n(\omega_i, T)$. Hence, the state $\hat{\rho}_{\mathrm{A}} \otimes \hat{\rho}'_{\mathrm{S}}$ is not entangled, and it does not have any quantum correlations. In another case, we can only obtain remaining qubits in a totally mixed state $\hat{\rho}_M = \hat{\rho}_{\mathrm{A}} \otimes \hat{\rho}'_{\mathrm{S}}$ which corresponds to no detected signal. Hypothesis H_0 takes the form:

$$\hat{\rho}_{H_0} = p\hat{\rho}_{\mathrm{A}} \otimes \hat{\rho}'_{\mathrm{S}} + (1-p)\hat{\rho}_M \tag{8}$$

where we have $\hat{\rho}_{\mathrm{A}} = \mathrm{Tr}_{\mathrm{S}}\{\hat{\rho}_{\mathrm{AS}}\} = \mathrm{diag}(a^2, b^2)$, $\hat{\rho}'_{\mathrm{S}} = \mathrm{Tr}_{\mathrm{A}}\{\hat{\rho}_{\mathrm{AS}}\} = \mathrm{diag}(b^2, a^2)$, $\hat{\rho}_M = \mathrm{diag}(a^2b^2, a^4, b^4, a^2b^2)$ with $\hat{\rho}_{\mathrm{AS}} = \hat{\rho}_{\mathrm{AS}}^{\Psi^\pm}$ from Equation (1a).

In Equation (8), parameter p depends on the emission frequency f and environment temperature T. Hypothesis H_0 is valid only if $f/T > \ln(2)k_B/h$ is true. As an example with $T = 20°\mathrm{C}$, the limiting frequency is $f \approx 4.23 \times 10^{12}\,\mathrm{Hz}$. Therefore, it includes as intended the microwave frequency range $I_\mu = [400\,\mathrm{kHz},\ 400\,\mathrm{GHz}]$ but not the optical range $I_{\mathrm{opt.}} = [3.75 \times 10^{14}, 7.5 \times 10^{14}]\,\mathrm{Hz}$.

Hypothesis H_1 corresponds to the presence of the target, so the emitted photon S can be potentially reflected by the object surface to the QI radar. We obtain the equation:

$$\hat{\rho}_{\mathrm{H}_1} = p\eta\hat{\rho}_{\mathrm{AS}} + (1-p\eta)\hat{\rho}_{\mathrm{A}} \otimes \hat{\rho}'_{\mathrm{S}} \tag{9}$$

where $\hat{\rho}_{\mathrm{AS}} = \hat{\rho}_{\mathrm{AS}}^{\Psi^\pm}$ from Equation (1a). In this equation, we take into consideration that we cannot distinguish the thermal photons of the polarization noise described in Equation (9), when the object is present but not detected. Then, we only keep one term for this situation. In Equation (9), we consider both the reflection probability η and thermal noise p. Consequently, hypothesis H_1 looks like a Werner state with a mixture of a maximally entangled state $\hat{\rho}_{\mathrm{AS}}$ and a totally mixed separable state $\hat{\rho}_{\mathrm{A}} \otimes \hat{\rho}'_{\mathrm{S}}$ [34]. This last state also represents the natural evolution of a quantum state in a perturbative medium like the atmosphere.

Considering both hypotheses H_0 and H_1, our binary decision strategy takes the form:

$$\hat{\Lambda} = \hat{\rho}_{H_1} - \hat{\rho}_{H_0} = p\eta\hat{\rho}_{\mathrm{AS}} + (1-p\eta)\hat{\rho}_{\mathrm{A}} \otimes \hat{\rho}'_{\mathrm{S}} - p\hat{\rho}_{\mathrm{A}} \otimes \hat{\rho}'_{\mathrm{S}} + (1-p)\hat{\rho}_M \tag{10}$$

Table 1. Conditional probabilities calculated using a projection measurement $\hat{P}_{HV}$ on $\hat{\Lambda}$.

Conditional probability	Situation of detection
$P(+\|\mathrm{H}_1) = p\eta a^2$	Detected object in hypothesis H_1
$P(-\|\mathrm{H}_1) = (1-p\eta)a^4$	Not-detected object in hypothesis H_1
$P(+\|\mathrm{H}_0) = pa^2b^2$	Detected object in hypothesis H_0
$P(-\|\mathrm{H}_0) = (1-p)a^2b^2$	Not-detected object in hypothesis H_0

Using $\hat{\Lambda}$, we make projection measurements $\{\hat{P}_{HH}, \hat{P}_{HV}, \hat{P}_{VH}, \hat{P}_{VV}\}$ in the eigenbasis of the two photons $\{|HH\rangle, |HV\rangle, |VH\rangle, |VV\rangle\}$ to compute conditional probabilities represented in Table 1 giving probabilities of detection. In this particular situation, we only made projection measurements on the eigenstate $|HV\rangle$. Using Table 1, we obtain the signal-to-noise ratios (SNR) of Equation (11).

$$\mathrm{SNR}_{H_1} = \frac{P(+|H_1)}{P(-|H_1)} = \frac{p\eta}{(1-p\eta)a^2} \tag{11a}$$

$$\mathrm{SNR}_{H_0} = \frac{P(+|H_0)}{P(-|H_0)} = \frac{p}{1-p} \tag{11b}$$

$$\mathrm{SNR}_{+} = \frac{P(+|H_1)}{P(+|H_0)} = \frac{\eta}{b^2} \tag{11c}$$

As in article [1], the number of entangled states represented by a, b improves the SNR. In Equation (11), only the SNR_{H_1} and SNR_{H_0} depend on the parameter p. However, the SNR_{+} does not clearly represent our decision strategy because the detection hypotheses do not discriminate the uncorrelated thermal photons of photon S from photon A kept inside the QI radar. It is a limitation of our detection model because SNR_{+} should depend on the thermal noise. Next, we only use formulas (11a) associated with a success probability and (11b) associated with a false alarm. They are represented in Figure 6. In this figure, we see that both SNR_{H_1} and SNR_{H_0} increase as the emission frequency increases. It respectively means that the success probability of detection grows as well as the false alarm probability. Nevertheless, we also obtain low SNR_{H_0} and SNR_{H_1} on the microwave range since $\mathrm{SNR}_{H_0}, \mathrm{SNR}_{H_1} < 1/2$, $\forall f \in [1, 1000]\,\mathrm{GHz}$. SNR_{H_0} only depends on p since the object is absent whereas the SNR_{H_1} depends on both p and η. It is the reflection probability η that permits to get a better success probability than the false alarm. In Figure 6, we can obtain $\mathrm{SNR}_{H_1} > \mathrm{SNR}_{H_0}$ only if $\eta \geqslant 0.52$. Hence, the reflection probability η plays an important role in this simple model of QI radar in polarization states.

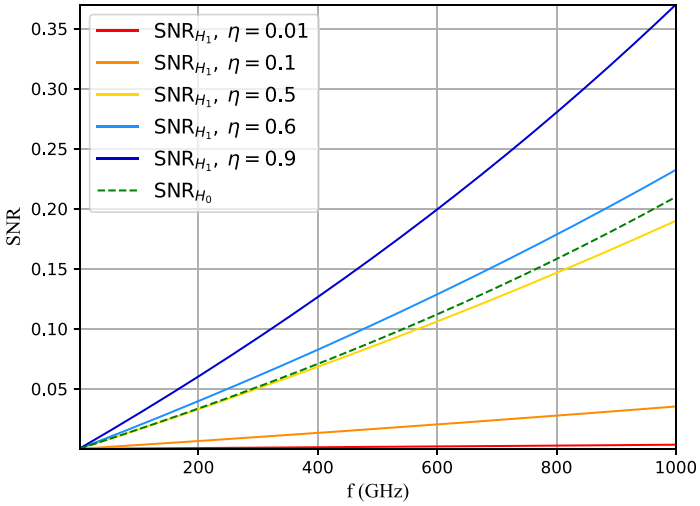

Figure 6. SNR_{H_1} and SNR_{H_0} with $a = b = 1/\sqrt{2}$ as function of the emitted frequency on a range $f \in [1, 1000]\,\mathrm{GHz}$ with 5 reflectivity coefficients from 0.01 to 0.9 for a temperature of $T = 300\,\mathrm{K}$.

According to these results, a QI radar in polarization states should take into consideration two major issues. On one hand, the microwave frequency regime around 10 GHz is suitable for the propagation distance of quantum correlations in the order of several kilometers. This is not the case anymore when we approach an emission frequency of 100 GHz or more. On the other hand, the great thermal noise around 10 GHz with more than 624 thermal qubits in average strongly limits the SNR for a reliable detection. However, SNR_{H_1} gets better when we increase the emission frequency whereas we lose range for quantum correlations. Taking these results into account, it seems clear that an optimization for the

emission frequency should be properly studied for a QI radar in the microwave regime in the atmosphere. We insist on the fact that our model is not realistic, but it highlights issues in microwave quantum radar theory.

Another issue is the independence of the channel influence γ from the detection strategy using p and η. Furthermore, in Equation (9) we did not clearly separate contributions of parameters η and p. Consequently, we attempt a new approach of the QI radar depicted in the next section where we combine the channel influence γ, reflection probability η, and thermal noise with p into a single model.

4.2. Alternative Detection Strategy

The objective of this second approach of the binary decision strategy is to discriminate the influence of the three parameters (γ, η, p) in the quantum radar scheme. We combine these three parameters into a single model of decision to make a link between the availability of quantum correlations and the binary decision strategy of the QI radar. For that, we modify the detection hypotheses H_0 and H_1 including the propagation model effects, and we compute the quantum discord on the detection hypotheses. Here, quantum discord does not represent the quantum correlations rate. It represents the distribution of quantum correlations in the decision strategy as function of (γ, η, p).

We rewrite the detection hypotheses H_0 and H_1. In hypothesis H_0, there is only the thermal noise, so the QI radar can only see one thermal qubit or nothing. Therefore, hypothesis H_0 of Equation (8) remains the same. Next, we modify hypothesis H_1. To study the influence of the parameters, we use a sum $\eta + p$ instead of the product ηp of Equation (9). We lose the physical description to separately study the influence of η, p, and γ. We obtain Equation (12):

$$\hat{\rho}_{H_1} \equiv \hat{\rho}_{\mathrm{AS}}^{(1)} = (\eta + p)\hat{\rho}_{\mathrm{AS,out}} + (1 - \eta - p)\hat{\rho}_{\mathrm{A}} \otimes \hat{\rho}_{\mathrm{S}} \tag{12}$$

On the left side, we have the quantum state $\hat{\rho}_{\mathrm{AS,out}}$ modified by the depolarizing channel of Equation (2). On the right side, we find the state product $\hat{\rho}_{\mathrm{A}} \otimes \hat{\rho}_{\mathrm{S}}$ where no object is detected. Notice that the modification of hypothesis H_1 involves the constraint $\eta + p < 1$ which limits the frequency range depending on the choice of η. Finally, in Equation (12) we obtain on the left an entangled quantum state that evolves thanks to the quantum channel action. On the right, we have a product state $\hat{\rho}_{\mathrm{A}} \otimes \hat{\rho}_{\mathrm{S}}$ corresponding to a not-entangled state of qubits A and S. It corresponds to the detection of photon S after it has been reflected by the target, or to a qubit S from the thermal noise.

Using these hypotheses H_0 and H_1, we write an operator $\hat{\Lambda}$ representing the binary decision strategy:

$$\hat{\Lambda} = \hat{\rho}_{H_1} - \hat{\rho}_{H_0} = (\eta + p)\hat{\rho}_{\mathrm{AS,out}} + (1 - \eta - p)\hat{\rho}_{\mathrm{A}} \otimes \hat{\rho}_{\mathrm{S}} - p\hat{\rho}_{\mathrm{A}} \otimes \hat{\rho}'_{\mathrm{S}} - (1 - p)\hat{\rho}_{M} \tag{13}$$

Equation (13) is written as function of (η, p) and γ with the operator $\hat{\rho}_{\mathrm{AS,out}}$. In $\hat{\Lambda}$, only the part $\hat{\rho}_{H_1} \equiv \hat{\rho}_{\mathrm{AS}}^{(1)}$ including the density operator $\hat{\rho}_{\mathrm{AS,out}}$ has some quantum information useful from the QI radar point of view. Consequently, to compute the distribution of quantum correlations we must calculate this distribution using the quantum discord over hypothesis H_1. So, we take Equation (12) for calculations where we only use $\hat{\rho}_{\mathrm{AS}}^{(1)}$ represented below:

$$\hat{\rho}_{\mathrm{AS}}^{(1)} = \begin{pmatrix} \rho_{11} & 0 & 0 & 0 \\ 0 & \rho_{22} & \rho_{23} & 0 \\ 0 & \rho_{32} & \rho_{33} & 0 \\ 0 & 0 & 0 & \rho_{44} \end{pmatrix} \tag{14}$$

where the coefficients $\{\rho_{ii}\}_{i=1\ldots4}$ verifying the condition $\mathrm{Tr}\{\hat{\rho}_{\mathrm{AS}}^{(1)}\} = \rho_{11} + \rho_{22} + \rho_{33} + \rho_{44} = 1$ are defined by:

$$\rho_{11} = (\eta + p)\frac{2}{3}\gamma a^2 + (1 - \eta - p)a^2 b^2 \tag{15a}$$

$$\rho_{22} = (\eta + p)(3 - 2\gamma)\frac{a^2}{3} + (1 - \eta - p)a^4 \tag{15b}$$

$$\rho_{23} = \rho_{32} = \pm(\eta + p)(3 - 4\gamma)\frac{ab}{3} \tag{15c}$$

$$\rho_{33} = (\eta + p)(3 - 2\gamma)\frac{b^2}{3} + (1 - \eta - p)b^4 \tag{15d}$$

$$\rho_{44} = (\eta + p)\frac{2}{3}\gamma b^2 + (1 - \eta - p)a^2 b^2 \tag{15e}$$

To compute the quantum discord $\delta(\hat{\rho}_{\mathrm{AS}}^{(1)})$ interpreted as a distribution of quantum correlations over hypothesis H_1, we first calculate the Von Neumann entropies (16a)–(16c).

$$\mathcal{S}(\hat{\rho}_{\mathrm{A}}^{(1)}) = (\rho_{11} + \rho_{22}) \log_2\left(\frac{1}{\rho_{11} + \rho_{22}}\right) + (\rho_{33} + \rho_{44}) \log_2\left(\frac{1}{\rho_{33} + \rho_{44}}\right) \tag{16a}$$

$$\mathcal{S}(\hat{\rho}_{\mathrm{S}}^{(1)}) = (\rho_{11} + \rho_{33}) \log_2\left(\frac{1}{\rho_{11} + \rho_{33}}\right) + (\rho_{22} + \rho_{44}) \log_2\left(\frac{1}{\rho_{22} + \rho_{44}}\right) \tag{16b}$$

$$\begin{aligned}\mathcal{S}(\hat{\rho}_{\mathrm{A}}^{(1)}|\hat{\rho}_{\mathrm{S}}^{(1)})_{\{\hat{M}_{\mathrm{S}}^{(i)}\}} = {} & \rho_{11} \log_2\left(\frac{\rho_{11} + \rho_{33}}{\rho_{11}}\right) + \rho_{33} \log_2\left(\frac{\rho_{11} + \rho_{33}}{\rho_{33}}\right) \\ & + \rho_{22} \log_2\left(\frac{\rho_{22} + \rho_{44}}{\rho_{22}}\right) + \rho_{44} \log_2\left(\frac{\rho_{22} + \rho_{44}}{\rho_{44}}\right)\end{aligned} \tag{16c}$$

where we observe that $\mathcal{S}(\hat{\rho}_{\mathrm{A}}^{(1)})$ does not explicitly depend on γ unlike $\mathcal{S}(\hat{\rho}_{\mathrm{S}}^{(1)})$ since the quantum channel only acts directly on the system S. We do not write here the calculus of the joint Von Neumann entropy $\mathcal{S}(\hat{\rho}_{\mathrm{AS}}^{(1)})$ which is quite long.

Using all these calculations, we obtain $\delta(\hat{\rho}_{\mathrm{AS}}^{(1)})$. As an example, in Figure 7(a) we represent the distribution of quantum correlations as function of γ for three different emission frequencies $f \in \{10, 50, 100\}$ GHz of the QI radar. We observe more quantum correlations for $\gamma = 0$ than $\gamma = 3/4$ since we are initially in the maximally entangled state $\hat{\rho}_{\mathrm{AS}}$ before the emission of photon S. Furthermore, we see that the greater the emission frequency is, the greater the quantum correlations for $\gamma = 0$ is. However, we have the same entangled quantum state at $\gamma = 0$ for each tested frequency. The slight difference is due to the probability p in Equation (12) which is weaker for $f = 100$ GHz than for $f = 10$ GHz. So, this increase is due to the contribution of η compared to p. It shows that the contribution of the parameter η of the target is important compared to the probability p. However, the difference between the values of $\delta(\hat{\rho}_{\mathrm{AS}}^{(1)})$ calculated for $\gamma = \{0, 3/4\}$ is around 0.02 bits which is relatively weak. According to Figure 7(a), we cannot conclude that calculations of the distribution of quantum

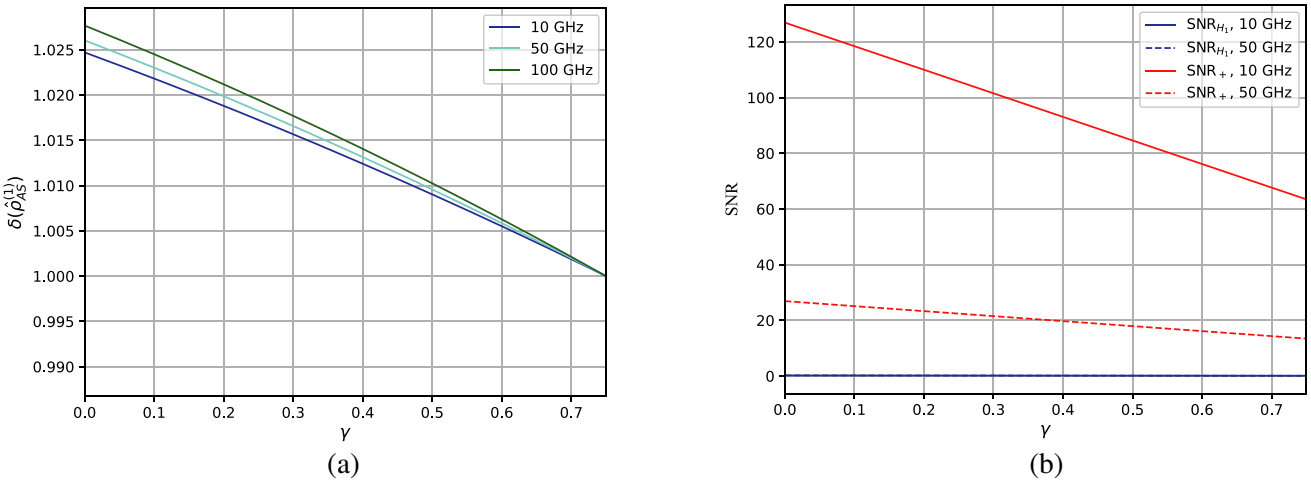

Figure 7. (a) Distribution of quantum correlations on hypothesis H_1 as function of the channel $\gamma \in [0, 3/4]$ for 3 different frequencies $f \in \{10, 50, 100\}$ GHz, for $\eta = 0.1$ and $a = b = 1/\sqrt{2}$. (b) $\mathrm{SNR}_{H_1}(|HV\rangle)$ and $\mathrm{SNR}_{+}(|HV\rangle)$ as function of $\gamma \in [0, 3/4]$, for $f \in \{10, 50\}$ GHz and $\eta = 0.1$ and $a = b = 1/\sqrt{2}$.

correlations with $\delta(\hat{\rho}_{\mathrm{AS}}^{(1)})$ can bring some useful information about the decision strategy in the QI radar as function of γ.

Additionally, if we compute $\delta(\hat{\rho}_{\mathrm{AS}}^{(1)})$ for two propagation parameters $\gamma = \{1/2, 3/4\}$ as function of η/p for $f = [5, 20]$ GHz using the same reflection coefficient $\eta = 0.1$, we obtain the same flat profile with roughly the same values. There is not any evolution of the distribution of quantum correlations as function of η/p. Consequently, this distribution as function of η/p cannot give any information about a potential optimization between η and p to use in this decision strategy of the QI radar.

Nevertheless, we must use the quantum discord $\delta(\hat{\rho}_{\mathrm{AS}}^{(1)})$ of hypothesis H_1 with the SNR calculated with the binary decision strategy of Equation (13).

Using Equation (13), we make projection measurements on the basis $\{|HH\rangle, |HV\rangle, |VH\rangle, |VV\rangle\}$ to obtain the SNR for hypotheses H_0 and H_1. The conditional probabilities are written in Table 2.

Table 2. Conditional probabilities calculated using a projection measurement on $\hat{\Lambda}$.

Conditional probability	$\|HH\rangle$	$\|HV\rangle$	$\|VH\rangle$	$\|VV\rangle$
$P(+\|\mathrm{H}_1)$	$(\eta+p)2/3\gamma a^2$	$(\eta+p)(3-2\gamma)a^2/3$	$(\eta+p)(3-2\gamma)b^2/3$	$(\eta+p)2/3\gamma b^2$
$P(-\|\mathrm{H}_1)$	$(1-\eta-p)a^2b^2$	$(1-\eta-p)a^4$	$(1-\eta-p)b^4$	$(1-\eta-p)a^2b^2$
$P(+\|\mathrm{H}_0)$	pa^2b^2	pa^4	pb^4	pa^2b^2
$P(-\|\mathrm{H}_0)$	$(1-p)a^2b^2$	$(1-p)a^4$	$(1-p)b^4$	$(1-p)a^2b^2$

For hypothesis H_0, we obtain the same SNR_{H_0} of Section 4.1 that is $\mathrm{SNR}_{H_0} = p/(1-p)$. For hypothesis H_1, we find the SNR_{H_1} written in Equation (17):

$$\mathrm{SNR}_{H_1}(|HH\rangle) = \frac{(\eta+p)\,2\gamma}{(1-\eta-p)\,3b^2} \tag{17a}$$

$$\mathrm{SNR}_{H_1}(|HV\rangle) = \frac{(\eta+p)\,(3-2\gamma)}{(1-\eta-p)\,3a^2} \tag{17b}$$

$$\mathrm{SNR}_{H_1}(|VH\rangle) = \frac{(\eta+p)\,(3-2\gamma)}{(1-\eta-p)\,3b^2} \tag{17c}$$

$$\mathrm{SNR}_{H_1}(|VV\rangle) = \frac{(\eta+p)\,2\gamma}{(1-\eta-p)\,3a^2} \tag{17d}$$

Then, we have also calculated the SNR_{+} in Equation (18):

$$\mathrm{SNR}_{+}(|HH\rangle) = \frac{(\eta+p)\,2\gamma}{3pb^2} \tag{18a}$$

$$\mathrm{SNR}_{+}(|HV\rangle) = \frac{(\eta+p)\,(3-2\gamma)}{3pa^2} \tag{18b}$$

$$\mathrm{SNR}_{+}(|VH\rangle) = \frac{(\eta+p)\,(3-2\gamma)}{3pb^2} \tag{18c}$$

$$\mathrm{SNR}_{+}(|VV\rangle) = \frac{(\eta+p)\,2\gamma}{3pa^2} \tag{18d}$$

All SNR_{H_1} and SNR_{+} are functions of (η, p, γ). In this binary decision strategy, we consider an initial quantum state $\hat{\rho}_{\mathrm{AS}} = |\Psi^+\rangle\langle\Psi^+|_{\mathrm{AS}}$ for the QI radar. We do not consider the $\mathrm{SNR}(|HH\rangle)$ and $\mathrm{SNR}(|VV\rangle)$ because $|HH\rangle$ and $|VV\rangle$ are not involved in the initial quantum state. Consequently, we do not take into account of Equations (17a), (17d), (18a), and (18d) because these SNRs increase since the evolution toward a maximally mixed state produces an overlap on $|HH\rangle$ and $|VV\rangle$. We set $a = b = 1/\sqrt{2}$ as follows.

Taking the SNR_{H_1} of Equation (17b), we look for a weak propagation $\gamma \ll 1$, we obtain $\mathrm{SNR}_{H_1} \approx 2(\eta + p)/(1 - \eta - p)$. To have an SNR greater than one, the contribution of the object with η must be greater than the noise with p. If we have $\eta \ll p$, then we would get $\mathrm{SNR}_{H_1} \approx 2p/(1-p)$ corresponding to the SNR_{H_0}. Hence, we would roughly have the same probability of success and false alarm which is not suitable for a radar application. On the contrary, for a long propagation $\gamma \to 1$, we obtain $\mathrm{SNR}_{H_1} \approx 2(\eta + p)/[3(1 - \eta - p)]$. There is a competition between contributions of parameters η and p in SNR_{H_1}. Moreover, we see that the quantum channel weakens the SNR_{H_1} with the factor $1/3$. However, we have mentioned earlier that the quantum channel does not permit to correctly follow the evolution of information with the binary decision strategy since we are limited to the range $\gamma \in [0, 3/4]$ in the quantum channel. This issue on the propagation model limits the validity of the SNR_{H_1} for a long propagation.

Next, we look for the SNR_+ in Equation (18b). For a low propagation $\gamma \ll 1$, we obtain $\mathrm{SNR}_+ \approx 2(\eta + p)/p$. We observe the enhancement in sensitivity thanks to the entanglement with factor 2. The SNR_+ depends on the competition between η and p for the SNR_{H_1}, and if $\eta \ll p$, only the entanglement gives an enhancement to the SNR_+. For a long propagation $\gamma \to 1$, we obtain $\mathrm{SNR}_+ \approx 2(\eta + p)/3p$. We have again the competition between η and p. If we have $\eta \ll p$, we have an SNR_+ depending on the entanglement with factor 2 and the quantum channel with factor $1/3$. The $\mathrm{SNR}_{+,\gamma\to 1} \approx 2/3 < 1$. We do not have an SNR equal to zero. The decision model needs improvements; however, it shows that the quantum channel plays a role in the decision strategy of the QI radar.

With both Equations (17b) and (18b), we obtain Figure 7(b) where we test two emission frequencies 10 GHz and 50 GHz. We note that the SNR_{H_1} is very low, close to zero for both emission frequencies whereas the SNR_+ takes values higher than one for both emission frequencies. However, in this figure, we do not distinguish the contributions of parameters η and p, making a confusion on the SNR meaning. However, Figure 7(b) highlights the role of the quantum channel in the decision strategy.

Looking at Figures 7(a) and 7(b) does not permit to make a clear link between the distribution of quantum correlations and the SNR calculated in Equations (17) and (18). If we have a slight decrease for the distribution of quantum correlations in Figure 7(a) and for the SNR_+ in Figure 7(b), we cannot conclude that the link is currently interesting to explore in this model.

5. CONCLUSION

In this work, we modeled the propagation of a photon in atmosphere while developing two approaches for the binary decision strategy of a QI radar using entanglement between qubits in polarization. We also made an estimation about the survival distance of entanglement and quantum correlations in the atmosphere. This estimation gives a survival distance of entanglement in the same order of magnitude of another article on this subject. Our model allows to give a trend about the survival distance for the entanglement and the discord as function of the emission frequency in the microwave frequency range.

For the two binary decision strategies tested, we attempted to make a link between the decision strategy and the propagation phase using a quantum channel. The first approach consists in making a decision strategy in parallel of the propagation phase modeling. It highlights a need to optimize the emission frequency to keep the quantum correlations as long as possible or to favour the signal-to-noise ratio. The second approach consists in exploring the distribution of quantum correlations in a new decision strategy separating the parameters of the quantum channel, object reflection, and channel influence. The last approach does not properly work since we cannot use it to better understand the link between quantum correlations and decision. However, it highlights that the quantum channel plays a role in the decision strategy with the SNR_{H_1} and SNR_+.

This paper gives an estimation about the entanglement and quantum correlations survival distances in the atmosphere. It also tries to link the decision strategy of the QI radar to the entanglement evolution. There are several possibilities to study the QI radar further.

First, we should work with more entangled photons taking into account more quantum states. The continuous variable formalism is suitable for this task, but it requires to use the quantum information theory in continuous variable [32]. Second, the used propagation model relies on a quantum channel using a classical attenuation model to estimate quantum correlation survival distances. This quantum channel provides a limited description of the propagation phase since we consider a

mean of all interactions between the emitted photon and atmospheric molecules. The study of these interactions is not in the scope of this paper. Thus, to improve the propagation model we should use a phenomenological model taking into account the influence of atmospheric molecules H_2O and O_2 as in the classical attenuation model. However, this new propagation model would be a quantum model considering all possible photon-molecule interactions which is a difficult task. We should also take into account other molecules like N_2. Such a phenomenological model is difficult to build and incorporate in the decision strategy of a QI radar. Third, the influence of the object surface must also be carefully studied. We must study the influence of non-homogeneous surfaces, the influence of volumes, and its effects on quantum information evolution.

At this stage of research, we cannot know whether a QI radar is feasible. There is still a lot of work to do on the quantum illumination protocol to develop further applications in remote sensing.

ACKNOWLEDGMENT

The research work has been carried out with the support of the AID-DGA (Defense Innovation Agency — French Ministry of the Armed Forces), and so the authors hereby wish to express their gratitude and thanks to the AID.

APPENDIX A. CALCULATION OF THE VON NEUMANN ENTROPIES TO EXPRESS THE QUANTUM DISCORD

We express the quantum discord $\delta(\hat{\rho}_{\mathrm{AS,\,out}})$ calculating the Von Neumann entropies of Equation (6b). For subsystems A and S, we have:

$$\mathcal{S}(\hat{\rho}_{\mathrm{A,\,out}}) = a^2 \log\left(\frac{1}{a^2}\right) + b^2 \log\left(\frac{1}{b^2}\right) \tag{A1a}$$

$$\begin{aligned}\mathcal{S}(\hat{\rho}_{\mathrm{S,\,out}}) = {} & \frac{(3-2\gamma)a^2+2\gamma b^2}{3} \log\left(\frac{3}{(3-2\gamma)a^2+2\gamma b^2}\right) \\ & + \frac{2\gamma a^2+(3-2\gamma)b^2}{3} \log\left(\frac{3}{2\gamma a^2+(3-2\gamma)b^2}\right)\end{aligned} \tag{A1b}$$

$\mathcal{S}(\hat{\rho}_{\mathrm{S,\,out}})$ explicitly depends on the quantum channel (2) since only photon S passes through the atmosphere. Next, we compute the conditional entropy with projection measurements on qubit S:

$$\begin{aligned}\mathcal{S}(\hat{\rho}_{\mathrm{A,\,out}}|\hat{\rho}_{\mathrm{S,\,out}})_{\{\hat{M}_S^{(i)}\}} = {} & \frac{2\gamma a^2}{3} \log\left(\frac{(3-2\gamma)b^2+2\gamma a^2}{2\gamma a^2}\right) + \frac{(3-2\gamma)b^2}{3} \log\left(\frac{2\gamma a^2+(3-2\gamma)b^2}{(3-2\gamma)b^2}\right) \\ & + \frac{(3-2\gamma)a^2}{3} \log\left(\frac{(3-2\gamma)a^2+2\gamma b^2}{(3-2\gamma)a^2}\right) + \frac{2\gamma b^2}{3} \log\left(\frac{(3-2\gamma)a^2+2\gamma b^2}{2\gamma b^2}\right)\end{aligned} \tag{A2}$$

Equation (A2) corresponds to the uncertainty on subsystem A when projection measurements are done on subsystem S.

Next, we compute the entropy of the system AS. The joint entropy $\mathcal{S}(\hat{\rho}_{\mathrm{AS,out}}) = -\mathrm{Tr}\{\hat{\rho}_{\mathrm{AS,out}} \log(\hat{\rho}_{\mathrm{AS,out}})\}$ is calculated by diagonalization of the matrix $\hat{\rho}_{\mathrm{AS,\,out}}$ to obtain an equation of the form $\log(\hat{\rho}_{\mathrm{AS,\,out}}) = P \log(D) P^{-1}$. So, we first get the eigenvalues of the density matrix $\hat{\rho}_{\mathrm{AS,out}}$:

$$\lambda_1 = \frac{2}{3}\gamma a^2; \quad \lambda_2 = \frac{2}{3}\gamma b^2; \quad \lambda_3 = \frac{3-2\gamma+3\sqrt{\Delta}}{6}; \quad \lambda_4 = \frac{3-2\gamma-3\sqrt{\Delta}}{6} \tag{A3}$$

where we have $\Delta = \frac{1}{9}[(1-4a^2b^2)(3-2\gamma)^2 + 4a^2b^2(3-4\gamma)^2]$ which equals zero only for $\gamma = 3/4$ for $\gamma \in [0,1]$. Now, depending on the Bell state $|\Psi^{\pm}\rangle_{\mathrm{AS}}$ or $|\Phi^{\pm}\rangle_{\mathrm{AS}}$, equations take different configurations, but we finally obtain the same result. We present the calculations for the states $|\Psi^{\pm}\rangle_{\mathrm{AS}}$. The operator $\hat{\rho}_{\mathrm{AS,out}} \log \hat{\rho}_{\mathrm{AS,out}}$ is written in Equation (A4).

$$\hat{\rho}_{\mathrm{AS,out}} \log \hat{\rho}_{\mathrm{AS,out}} = \begin{pmatrix} H_1 & 0 & 0 & 0 \\ 0 & H_2 & \pm H_3 & 0 \\ 0 & \pm H_4 & H_5 & 0 \\ 0 & 0 & 0 & H_6 \end{pmatrix} \tag{A4}$$

where the coefficients $H_{i=1...6}$ are defined in Equation (A5).

$$H_1 = \frac{2}{3}\gamma a^2 L_1 \tag{A5a}$$

$$H_2 = (3-2\gamma)\frac{a^2}{3}L_2 + (3-4\gamma)\frac{ab}{3}L_4 \tag{A5b}$$

$$H_3 = (3-2\gamma)\frac{a^2}{3}L_3 + (3-4\gamma)\frac{ab}{3}L_5 \tag{A5c}$$

$$H_4 = (3-4\gamma)\frac{ab}{3}L_2 + (3-2\gamma)\frac{b^2}{3}L_4 \tag{A5d}$$

$$H_5 = (3-4\gamma)\frac{ab}{3}L_3 + (3-2\gamma)\frac{b^2}{3}L_5 \tag{A5e}$$

$$H_6 = \frac{2}{3}\gamma b^2 L_6 \tag{A5f}$$

and the coefficients $L_{i=1...6}$ are:

$$L_1 = \log(\lambda_1) \tag{A6a}$$

$$L_2 = \frac{1}{c_2 d_1 - c_1 d_2}\left(c_2 d_1 \log(\lambda_4) - c_1 d_2 \log(\lambda_3)\right) \tag{A6b}$$

$$L_3 = \frac{c_1 d_1}{c_2 d_1 - c_1 d_2}\left(\log(\lambda_4) - \log(\lambda_3)\right) \tag{A6c}$$

$$L_4 = \frac{c_2 d_2}{c_2 d_1 - c_1 d_2}\left(\log(\lambda_3) - \log(\lambda_4)\right) \tag{A6d}$$

$$L_5 = \frac{1}{c_2 d_1 - c_1 d_2}\left(c_2 d_1 \log(\lambda_3) - c_1 d_2 \log(\lambda_4)\right) \tag{A6e}$$

$$L_6 = \log(\lambda_2) \tag{A6f}$$

The coefficients L_i are defined as function of $c_{i=1,2}$, $d_{i=1,2}$:

$$c_1 = \frac{2(3-4\gamma)ab}{\sqrt{4(3-4\gamma)^2a^2b^2 + [(3-2\gamma)(2a^2-1) - 3\sqrt{\Delta}\,]^2}} \tag{A7a}$$

$$c_2 = \frac{(3-2\gamma)(2a^2-1) - 3\sqrt{\Delta}}{\sqrt{4(3-4\gamma)^2a^2b^2 + [(3-2\gamma)(2a^2-1) - 3\sqrt{\Delta}\,]^2}} \tag{A7b}$$

$$d_1 = \frac{2(3-4\gamma)ab}{\sqrt{4(3-4\gamma)^2a^2b^2 + [(3-2\gamma)(2a^2-1) + 3\sqrt{\Delta}\,]^2}} \tag{A7c}$$

$$d_2 = \frac{(3-2\gamma)(2a^2-1) + 3\sqrt{\Delta}}{\sqrt{4(3-4\gamma)^2a^2b^2 + [(3-2\gamma)(2a^2-1) + 3\sqrt{\Delta}\,]^2}} \tag{A7d}$$

Finally, we obtain the joint Von Neumann entropy $\mathcal{S}(\hat{\rho}^{\Psi^\pm}_{\mathrm{AS,out}}) = -H_1 - H_2 - H_5 - H_6$. Using Equations (A1)–(A7), we obtain the quantum discord $\delta(\hat{\rho}_{\mathrm{AS,out}})$ represented in Figure 2.

REFERENCES

1. Lloyd, S., "Enhanced sensitivity of photodetection via quantum illumination," *Science*, Vol. 321, No. 5895, 1463–1465, September 2008.
2. Tan, S.-H., B. I. Erkmen, V. Giovannetti, S. Guha, S. Lloyd, L. Maccone, S. Pirandola, and J. H. Shapiro, "Quantum illumination with Gaussian states," *Physical Review Letters*, Vol. 101, No. 25, 253601, December 2008.

3. Sorelli, G., N. Treps, F. Grosshans, and F. Boust, "Detecting a target with quantum entanglement," *IEEE Aerospace and Electronic Systems Magazine*, 2021.
4. Shapiro, J. H., "The quantum illumination story," *arXiv:1910.12277 [quant-ph]*, December 2019, arXiv: 1910.12277.
5. Shapiro, J. H., "Microwave quantum radar's alphabet soup: QI, QI-MPA, QCN, QCN-CR," *2021 IEEE Radar Conference (RadarConf21)*, 1–6, IEEE, Atlanta, GA, USA, May 2021.
6. Torrome, R. G., N. B. Bekhti-Winkel, and P. Knott, "Quantum illumination with multiple entangled photons," *Advanced Quantum Technologies*, Vol. 4, No. 11, 2100101, November 2021, arXiv:2008.09455 [quant-ph].
7. Zhang, Z., S. Mouradian, F. N. C. Wong, and J. H. Shapiro, "Entanglement enchanced sensing in a lossy and noisy environment," *Physical Review Letters*, Vol. 114, No. 11, 110506, March 2015.
8. Lopaeva, E. D., I. Ruo Berchera, I. P. Degiovanni, S. Olivares, G. Brida, and M. Genovese, "Experimental realization of quantum illumination," *Physical Review Letters*, Vol. 110, No. 15, 153603, April 2013.
9. Fasolo, L., A. Greco, E. Enrico, F. Illuminati, R. L. Franco, D. Vitali, and P. Livreri, "Traveling wave parametric amplifiers as non-classical light source for microwave quantum illumination," *Measurement: Sensors*, Vol. 18, 100349, December 2021.
10. Barzanjeh, Sh., M. Abdi, G. J. Milburn, P. Tombesi, and D. Vitali, "Reversible optical to microwave quantum interface," *Physical Review Letters*, Vol. 109, No. 13, 130503, September 2012, arXiv: 1110.6215.
11. Livreri, P., E. Enrico, L. Fasolo, A. Greco, A. Rettaroli, D. Vitali, A. Farina, F. Marchetti, and D. Giacomin, "Microwave quantum radar using a Josephson traveling wave parametric amplifier," *2022 IEEE Radar Conference (RadarConf22)*, 1–5, IEEE, New York City, NY, USA, March 2022.
12. Barzanjeh, S., S. Pirandola, D. Vitali, and J. M. Fink, "Microwave quantum illumination using a digital receiver," *Science Advances*, Vol. 6, No. 19, eabb0451, May 2020.
13. Barzanjeh, S., M. C. de Oliveira, and S. Pirandola, "Microwave photodetection with electro-opto-mechanical systems," *arXiv:1410.4024 [quant-ph]*, October 2014, arXiv: 1410.4024.
14. Jo, Y., S. Lee, Y. S. Ihn, Z. Kim, and S.-Y. Lee, "Quantum illumination receiver using double homodyne detection," *Physical Review Research*, Vol. 3, No. 1, 013006, January 2021.
15. Weedbrook, C., S. Pirandola, J. Thompson, V. Vedral, and M. Gu, "How discord underlies the noise resilience of quantum illumination," *New Journal of Physics*, Vol. 18, No. 4, 043027, April 2016, arXiv: 1312.3332.
16. Wilde, M., *Quantum Information Theory*, 2nd Edition, Cambridge University Press, Cambridge, UK; New York, OCLC: ocn973404322, 2017.
17. Hayashi, M., S. Ishizaka, A. Kawachi, G. Kimura, and T. Ogawa, "Introduction to quantum information science," *Graduate Texts in Physics*, Springer Berlin Heidelberg, Berlin, Heidelberg, 2015.
18. Ollivier, H. and W. H. Zurek, "Quantum discord: A measure of the quantumness of correlations," *Physical Review Letters*, Vol. 88, No. 1, 017901, December 2001.
19. Streltsov, A., *Quantum Correlations beyond Entanglement*, Springer Briefs in Physics, Springer International Publishing, Cham, 2015.
20. Emary, C., B. Trauzettel, and C. W. J. Beenakker, "Entangled microwave photons from quantum dots," *Physical Review Letters*, Vol. 95, No. 12, 127401, September 2005, arXiv:cond-mat/0502550.
21. Kumano, H., K. Matsuda, S. Ekuni, H. Sasakura, and I. Suemune, "Characterization of two-photon polarization mixed states generated from entangled-classical hybrid photon source," *Optics Express*, Vol. 19, No. 15, 14249, July 2011.
22. Brandsema, M. J., R. M. Narayanan, and M. Lanzagorta, "Theoretical and computational analysis of the quantum radar cross section for simple geometrical targets," *Quantum Information Processing*, Vol. 16, No. 1, 32, January 2017.
23. Brandsema, M. J., "Formulation and analysis of the quantum radar cross section," PhD thesis, Pennsylvania State University, United States, 2017.

24. Bavontaweepanya, R., "Effect of depolarizing noise on entangled photons," *Journal of Physics: Conference Series*, Vol. 1144, 012047, December 2018.
25. He, J. and L. Ye, "Protecting entanglement under depolarizing noise environment by using weak measurements," *Physica A: Statistical Mechanics and Its Applications*, Vol. 419, 7–13, February 2015.
26. Dehmani, M., H. Ez-Zahraouy, and A. Benyoussef, "Transmissions of quantum entangled states in anisotropic depolarizing channels," *Journal of Russian Laser Research*, Vol. 34, No. 1, 71–76, January 2013.
27. Sk, R. and P. K. Panigrahi, "Protecting quantum coherence and entanglement in a correlated environment," *Physica A: Statistical Mechanics and Its Applications*, Vol. 596, 127129, June 2022.
28. Wootters, W. K., "Entanglement of formation of an arbitrary state of two qubits," *Physical Review Letters*, Vol. 80, No. 10, 2245–2248, March 1998, arXiv: quant-ph/9709029.
29. Henderson, L. and V. Vedral, "Classical, quantum and total correlations," *Journal of Physics A: Mathematical and General*, Vol. 34, No. 35, 6899–6905, September 2001, arXiv: quant-ph/0105028.
30. Liebe, H. J., "An updated model for millimeter wave propagation in moist air," *Radio Science*, Vol. 20, No. 5, 1069–1089, September 1985.
31. Li, X., D.-W. Wu, C.-Y. Yang, W.-L. Li, and Q. Miao, "Quantitative analysis of decoherence of entangled microwave signals in free space," *Quantum Information Processing*, Vol. 18, No. 7, 200, July 2019.
32. Navarrete-Benlloch, C., "An introduction to the formalism of quantum information with continuous variables," *IOP Concise Physics*, Morgan & Claypool, USA, 2015.
33. Helstrom, C. W., *Quantum Detection and Estimation Theory*, Academic Press, New York, 1976.
34. Werner, R. F., "Quantum states with Einstein-Podolsky-Rosen correlations admitting a hidden variable model," *Physical Review A*, Vol. 40, No. 8, 4277–4281, October 1989.